Available online at www.sciencedirect.com
SCIENCE DIRECT®
Journal of Chromatography B, 793 (2003) 229–251
JOURNAL OF CHROMATOGRAPHY B
www.elsevier.com/locate/chromb

Imaging surface plasmon resonance system for screening affinity ligands

Paul R. Morrill[1], R.B. Millington[2], Christopher R. Lowe*

Institute of Biotechnology, University of Cambridge, Tennis Court Road, Cambridge CB2 1QT, UK

Received 25 November 2002; received in revised form 28 March 2003; accepted 31 March 2003

Abstract

A surface plasmon resonance (SPR) system for screening ligands for application in affinity chromatography is described. A combinatorial library of 13 ligands was synthesised, characterised and immobilised to agarose beads and gold SPR devices. Binding and elution behaviour and a range of K_{AX} values (10^3 to 10^5 M^{-1}) were measured against two target proteins, an insulin analogue (MI3) and a recombinant clotting factor (rFVIIa), in order to create a relational database between the traditional chromatographic format and the new SPR screening system. The SPR transducer surface was fabricated with affinity ligands in a two-dimensional, spatially addressable format, which was durable (>100 cycles) and stable over 6 months. The imaging SPR system comprised a direct optical, CCD-based, instrument capable of imaging the change in refractive index created by biochemical interactions and allowed affinity ligands to be evaluated 15-fold faster with 130-fold less target protein than conventional chromatographic methods. The binding and elution data from both the SPR and chromatographic systems for both target proteins were comparable, with the K_{AX} value generating a nearly linear correlation (R^2=0.875) and a slope bias of ~2.5±0.25-fold higher for the SPR system. The imaging SPR system has proven capable of screening and evaluating affinity ligands for potential use in the recovery of biopharmaceutical proteins.

Keywords: Surface plasmon resonance; Affinity ligands

1. Introduction

The ability to produce substantial quantities of pure, safe and effective therapeutic proteins from transgenic organisms is an on-going challenge. The impact of human genomics and proteomics, together with cost containment in healthcare management, environmental and safety legislation, and the appearance of generic biopharmaceuticals, is likely to drive the pharmaceutical industry towards the introduction of high throughput, cost effective and flexible manufacturing processes based on new technologies [1,2]. Highly selective techniques such as affinity chromatography are expected to play an increasing role in bioprocessing, since, not only does the methodology satisfy the requirement for resolving the target protein from other inert and host proteins present in the expression system, but it is also capable of

*Corresponding author. Tel.: +44-223-334-160; fax: +44-223-334-162.
E-mail address: crl1@biotech.cam.ac.uk (C.R. Lowe).
[1]Present address: Acumen Bioscience Ltd., Melbourn Science Park, Cambridge Road, Melbourn, Royston, Herts. SG8 6EE, UK.
[2]Present address: OptoPhysics, 28, Grasmere, Huntingdon, Cambridgeshire PE18 6UR, UK.

1570-0232/03/$ – see front matter
doi:10.1016/S1570-0232(03)00282-4

removing bioactive contaminants and structural isoforms of the target protein, thereby providing in-built quality assurance. High-capacity synthetic affinity adsorbents which are able to adsorb and elute native proteins in high yield and are capable of withstanding the rigours of harsh manufacturing protocols are now available [3–8].

Computer-aided molecular modelling has been used extensively to design customised ligands, where a suitable template structure is derived from known ligands [8,9] or complementary binding molecules [3,4]. However, selection of a target site and the design, synthesis and evaluation of an affinity ligand is, at best, a semi-rational process. Ligand immobilisation to a solid phase introduces a plethora of unknown factors determined partly by the chemical and spatial characteristics of the ligand per se and partly by features of the matrix, spacer and scaffold groups and the activation and coupling chemistries. Furthermore, ligand selection by screening interactions between soluble ligands and the target protein are not representative of the complex environment created by the chemical, geometrical and steric constraints imposed by the three-dimensional matrix. Consequently, structural knowledge of the target protein coupled with combinatorial ligand libraries and effective screening protocols has been used recently to create effective affinity adsorbents [1,7,10,11].

This new strategy dramatically reduces the time taken to identify a site on the target protein and procure a viable ligand, although it still suffers from using traditional time-consuming chromatographic methods, which require relatively large quantities of expensive target proteins to assess performance. In order to address this problem, a new strategy is required that would enable the rapid evaluation of the performance of putative affinity adsorbents. Determination of the association equilibrium constant (K_{AX}) and binding and elution profiles for the target protein are required to assess whether an affinity ligand is suitable for use in a commercial process. It is envisaged that simple, robust and inexpensive biosensor techniques could be developed in a miniaturised, automated format and integrated with liquid handling in order to read multiple samples in parallel. This system would facilitate the rapid and efficient evaluation of libraries of biomimetic ligands, using relatively small quantities of the target proteins, and generate a structure–activity relationship (SAR) database that could allow a truly adaptive high throughput screening methodology to be applied for the first time to affinity ligands [12–14].

A number of transducers are suitable for incorporation into affinity sensors [15,16], although the most widely employed are those that exploit the sensitivity of surface plasmons to changes in dielectric permittivity at a metal interface [17–19]. Surface plasmon resonance (SPR) is a robust technique that has a proven ability to detect biological compounds in the nM–μM concentration range in real-time without additional secondary labelling of the target protein [20–24]. From early fundamental studies [25–27], SPR has grown into a technique that is versatile and amenable to a variety of applications, including absorbance monitoring [28], biokinetic studies [29,30] biosensing and gas detection [17,22], bulk liquid measurements [31], immunosensing [32], light modulation [33], SPR microscopy [34,35], refractive index measurements [28], SPR polarisation [36] and thin film characterisation [37].

Custom designed biomimetic affinity ligands have been exploited in the creation of a new class of highly selective, stable and regenerable affinity sensors for application in in situ bioprocess monitoring [38]. These molecules do not suffer from changes in activity on immobilisation and are readily configurable into highly ordered two- and three-dimensional ligand arrays on the sensor surface. Binding of the target protein is usually reversible, thereby allowing regeneration and re-sterilisation of the sensor surface, and resulting in a prolonged shelf life for the sensor. This report describes work aimed at developing an imaging SPR instrument able to monitor interactions between two target proteins, an insulin analogue, MI3 [1], and recombinant clotting factor VIIa (rFVIIa) [10], and a library of defined triazine ligands designed to bind differentially to the two proteins.

2. Experimental

2.1. Chemicals

Acetic acid, acetone, 3-aminobenzoic acid, 2-aminobenzimidazole, 6-aminocaproic acid, 2-amino-

indan, 3-amino-2-naphthoic acid, 1-amino-5-naphthol, 4-amino-1-naphthol, 3-aminophenol, ammonia, ammonium cerium nitrate, benzylamine, 3,5-diaminobenzoic acid, dichloromethane (DCM, HPLC grade), dimethylformamide (DMF, HPLC grade), dimethylsulfoxide (DMSO, HPLC grade), epichlorohydrin, ethanol, ethyl acetate, ethylenediaminetetracetic acid (EDTA), hexane, hydrochloric acid, hydrogen peroxide, mercaptoethanol, 11-mercapto-1-undecanol, methanol, 1-naphthylacetonitrile, nitric acid, ninhydrin, light petroleum 80–100 °C, propan-2-ol, sodium hydrogencarbonate, sodium carbonate, sodium chloride, sodium hydroxide, sodium phosphate, sodium tetraborate, 1,3,5-trichlorotriazine, 2,4,6-trinitrobenzenesulfonic acid (TNBS) and tyramine were all purchased from Aldrich (Gillingham, UK). Calcium chloride and trizma base [tris(hydroxymethyl)aminomethane] were purchased from Sigma (Poole, UK). 1-Amino-6-naphthalene sulfonic acid was purchased from Lancaster Synthesis (Morecambe, UK). 1-Amino-7-naphthol, 2-amino-1-naphthol and 6-amino-1-naphthol were purchased from TCI Tokyo, Kasei Kogyo (Tokyo, Japan). Coomassie Brilliant Blue G-250 solution and Iodo-Beads were purchased from Pierce Immunochemicals (Rockford, IL, USA). Dextran T-500 was purchased from Pharmacia Fine Chemicals (Uppsala, Sweden).

All chemicals were of general purpose reagent grade unless otherwise stated. All solutions, washes, and procedures that required water utilised high purity (18 MΩ/cm) water from an Elgastat water purification system at the Institute of Biotechnology (Cambridge, UK).

2.2. Biochemicals

Recombinant insulin precursor (MI3; M_r 5956) and recombinant blood coagulation Factor VII (rFVIIa; M_r 50 000), were kindly supplied by Novo Nordisk (Gentofte, Denmark). Samples had been tested for purity and biological efficacy by the quality control department (QC) of Novo Nordisk. Bovine serum albumin (BSA) was purchased from Sigma.

2.3. Chromatographic materials

Pre-packed Sephadex G-25 (PD-10) desalting columns and HR 5/2 columns were purchased from Pharmacia Biotechnology (Uppsala, Sweden). Polypropylene columns (4 ml) and frits, for screening purposes, were purchased from Varian (Surrey, UK). Analytical thin-layer chromatography (TLC) plates, coated with 0.25 mm silica gel containing UV 254 nm fluorescent indicator, were purchased from Macherey–Nagel (Duren, Germany). Glass capillary tubes, used for spotting samples, were hand drawn using pasteur pipettes purchased from John Poulten (Essex, UK). Sepharose CL-6B was purchased from Pharmacia Biotechnology.

2.4. Radiochemicals

Iodine isotope 125 (I^{125}, 20 mCi) in carrier-free sodium iodide (NaI), radioactive protective screen, storage box, working trays and protective lead apron were all purchased from Amersham International (Buckinghamshire, UK).

2.5. Other materials

The perspex immobilisation block was fabricated by the Engineering Department (Cambridge University, UK). Viton [poly(hexafluoro)propylene–co-vinylidine fluoride] O-rings of 6.8 mm I.D. and a wall thickness of 1.6 mm were purchased from Mecro (UK). Poly vinyl chloride (PVC) tubing (1 mm I.D.) was purchased from Anachem (Luton, UK). SPR glass prisms, optical grade SF11 (refractive index 1.78), were purchased from Comar (Cambridge, UK). SPR glass slides, optical grade SF2 (refractive index 1.65), were purchased from UQG Optical Components (Cambridge, UK). Chromium plated tungsten rods were obtained from Megatech (Hantsuk, UK). Gold powder Puratronic 20 mesh (99.9995% pure) was purchased from Alfa (Karlsruhe, Germany).

2.6. Solution phase synthesis and immobilisation of triazine ligands

Cyanuric chloride (30 g, 0.16 mol) was recrystallised by dissolution in 500 ml hot (90 °C) light petroleum (80–100 °C boiling point), filtering hot and leaving the saturated cyanuric chloride solution overnight in the fume hood to allow crystal forma-

tion. The crystals were collected, dried under reduced pressure, and stored in an airtight container at room temperature until required. Crystals of cyanuric chloride in 80% yield with a melting point of 145 °C were obtained.

A fine slurry of cyanuric chloride was prepared by adding a solution of recrystallised cyanuric chloride (1106 mg, 6 mmol) in acetone (24 ml) into well stirred ice-water. A solution of the first amino substituent (6 mmol) in acetone (10 ml) together with $NaHCO_3$ (504 mg, 6 mmol) in water (10 ml) was added and allowed to mix at 0 °C for approximately 2 h. The progress of the reaction was checked by TLC to ensure complete reaction. The solid was filtered on a büchner funnel containing ashless filter paper (42 grade, 5.5 cm), washed with copious amounts of water and dried in vacuo over KOH for approximately 12 h. The product was weighed for yield and TLC and mass spectrometry (MS) performed to assess product purity and mass.

The product recovered from the first substitution (1 mmol) was dissolved in acetone (4 ml) and added to water (6 ml) at 40 °C. To this suspension, the second amino substituent (1 mmol) in acetone (2 ml) together with Na_2CO_3 (1 mmol) in water (2 ml) was added and allowed to react at 40 °C for a total of 12 h. The progress of the reaction was checked by TLC until only bis-substituted triazine could be detected, whence the product was precipitated from the reaction mixture by the addition of 1 *M* HCl and water. The solid was filtered on a büchner funnel containing ashless filter paper (42 grade, 5.5 cm), washed with copious amounts of water and dried in vacuo over KOH for approximately 12 h. The product was weighed for yield, TLC and MS performed to assess product purity and mass.

2.7. Ligand immobilisation on agarose

Sepharose CL-6B (100 g) was washed thoroughly with distilled water on a sintered glass funnel, transferred to a conical flask and suspended in 10 *M* NaOH (8 ml) and water (64 ml). To this suspension, epichlorohydrin (7.2 ml) was added and allowed to react at 30 °C for 100 min with gentle agitation. Upon completion of the initial activation step, the slurry was washed extensively with mixtures of acetone–water (1:2, 1:1, 2:1, 1:0, 2:1, 1:1, 1:2, 0:1, v/v). The activated agarose was stored in 20% (v/v) ethanol at 4 °C until required.

The extent of epoxide activation was determined by thoroughly washing a portion of reacted gel with water (1 ml), adding 1.3 *M* sodium thiosulfate (3 ml) and allowing to stand at room temperature for approximately 20 min. While monitoring the pH, 0.1 *M* HCl was titrated into the solution until pH 7 was reached. The epoxide content was determined by the volume (μl) of HCl added divided by 10 and expressed as (μmol epoxide groups/g moist mass gel).

2.8. Chromatographic evaluation of immobilised ligands

Stock solutions of the target proteins were prepared as follows: MI3 paste (~50%, w/w, MI3; lot No. QC206860) was weighed (400 mg) into a beaker, whence 0.1 *M* acetic acid (25 ml) was added and allowed to mix. The pH of the solution was adjusted to 3.0 until the MI3 paste had completely dissolved followed by an additional pH adjustment to a final value of 4.5. The concentration of the MI3 stock solution was approximately 4 mg/ml (670 μ*M*), portioned in aliquots (5 ml) and frozen at −20 °C until required. Purified rFVIIa (lot No. RENS7; 1.52 mg/ml) was exchanged on G-25 (PD-10) columns [previously equilibrated with 20 m*M* Tris, 50 m*M* NaCl, 2.5 m*M* calcium chloride, pH 8.0; 30 column volumes (binding buffer)] by adding the purified protein (2.5 ml) onto the column and eluting with binding buffer (3.5 ml). This procedure was repeated as necessary to exchange the amount of rFVIIa required to complete the experiments. The concentration of the rFVIIa solution was approximately 1 mg/ml (20 μ*M*), portioned in aliquots (5 ml) and frozen at −20 °C until required.

Each affinity gel (17.5 μmol ligand/g moist mass gel) prepared from the ligands listed in Table 1 was packed (1 ml) in polypropylene columns (4 ml) between 20 μm frits. The columns were washed with regeneration buffer (30%, v/v, isopropanol, 0.2 *M* NaOH) until no ligand leakage was detected by 254 nm and then with water (10 column volumes). In the case of MI3, the columns were equilibrated with binding buffer (0.1 *M* sodium acetate, pH 4.5; 30 column volumes) whence MI3 (1 mg/ml in binding

Table 1
Amines used for the construction of the MI3 and FVIIa library

NO	AMINE	STRUCTURE	NO	AMINE	STRUCTURE
1	1-Amino-6-naphthalene sulphonic acid	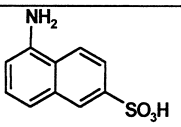	19	4-Amino-1-naphthol	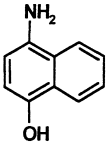
2	1-Amino-5-naphthol	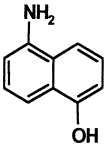	23	1-Amino-7-naphthol	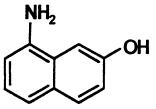
3	Benzylamine	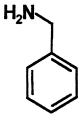	24	2-Amino-1-naphthol	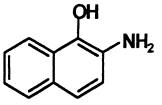
4	3,5-Diamino-benzoic acid	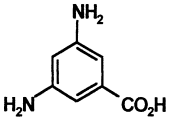	25	6-Amino-1-naphthol	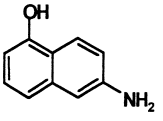
5	3-Aminobenzoic acid	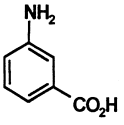	28	2-Aminobenzimidazole	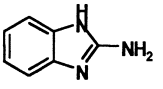
7	Tyramine	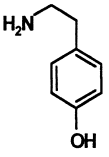	42	5-Aminoindan	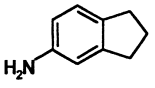
15	3-Amino phenol	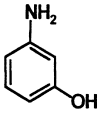			
18	3-Amino-2-naphthol	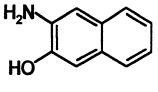			

buffer; 1 ml) was applied. The columns were washed with binding buffer (10 ml total in 1 ml aliquots) followed by elution with elution buffer (2 *M* acetic acid; 3 ml total in 1 ml aliquots). The sample, flow through and elution fractions were collected from each column and analysed for the presence of MI3 utilising the known extinction coefficient of the protein.

For rFVIIa, the columns were equilibrated with binding buffer (20 m*M* Tris–HCl, 50 m*M* NaCl, 2.5

m*M* calcium chloride, pH 8.0; 30 column volumes) whence rFVIIa (1 mg/ml in binding buffer; 1 ml) was applied. The columns were washed with binding buffer (10 ml in 1 ml aliquots) followed by elution with elution buffer (20 m*M* Tris–HCl, 50 m*M* NaCl, 5 m*M* EDTA, pH 7.5; 3 ml total in 1 ml aliquots). The sample, flow through and elution fractions were collected for each column and analysed for the presence of rFVIIa utilising the known extinction coefficient of the protein.

After use, all columns were treated with regeneration buffer followed by water before being stored in 20% (v/v) ethanol.

2.9. Determination of the association equilibrium constant (K_{AX})

Each affinity gel prepared from the ligands listed in Table 1 was dried on a No. 3 sinter funnel, weighed (0.2 g), rehydrated in water (approximate bed volume 0.325 ml) and packed in a HR 5/2 (Pharmacia) column. The columns were equilibrated with binding buffer (30 column volumes) on a BioCad 700E workstation prior to evaluation. Purified MI3 (0–4 mg/ml; 15 ml) or rFVIIa (0–1 mg/ml; 15 ml) was applied through a sample loop (15 ml) at a flow-rate of 0.3 ml/min, whence the regeneration buffer was applied at 0.3 ml/min (30 column volumes) followed by binding buffer. The frontal chromatograms were monitored with a UV detector set at 280 nm. From the breakthrough curves generated at each MI3 or rFVIIa concentration in triplicate, 50% of the absorbance at steady state was used to determine the elution volume of MI3 or rFVIIa ($\overline{V}_A$). The column bed volume (V_A^*) was determined by using the same gel volume of unmodified matrix and determining the breakthrough curve of MI3 (2 mg/ml) or rFVIIa (1 mg/ml). The association equilibrium constant (K_{AX}) was determined from the resulting Scatchard plot according to the method of Winzor [39].

2.10. Cleaning of SPR glass slides and prisms

The cleaning protocol for SPR glass slides and prisms consisted of two parts: (A) removal of the gold and chromium, comprised the following steps: (1) sonication in the Lucas Dawe sonication bath at 25 °C in hydrochloric acid–nitric acid, 3:1, v/v, for 5 min, followed by extensive rinsing in distilled water; (2) further sonication at 25 °C in 1 *M* ammonium cerium nitrate solution for 5 min, followed by extensive rinsing in distilled water. (B) Cleaning of the glass surfaces, comprised the following steps: (1) incubation in sulfuric acid–hydrogen peroxide, 1:1 (Piranha Solution) for 10 min at 25 °C, followed by extensive rinsing in distilled water; (2) sonication in propan-2-ol at 25 °C for 10 min, followed by oven drying at 50 °C until thoroughly dry (approximately 10–15 min).

2.11. Deposition of gold films on SPR glass slides and prisms

A thermal evaporation technique was used to deposit the chromium and gold onto the glass surfaces. After cleaning, the glass slides or prisms were placed within the deposition chamber of the Edwards E306B. Deposition of a 2 nm chromium adhesion layer followed by a 50 nm gold layer was accomplished by reducing the chamber pressure below $3 \cdot 10^{-6}$ Torr, setting the deposition rate to approximately 5 Å/s and a substrate temperature of 25 °C (1 Torr=133.322 Pa). Samples were allowed to cool within the chamber for 1 h when they were either reacted with a surface chemistry or stored in a vacuum dessicator under nitrogen until required.

2.12. SPR sensor fabrication

All ligands within the library (0.12 mmol) were dissolved in DMF (4 ml), 2-aminoethanethiol hydrochloride (18.51 mg; 0.240 mmol) and $NaHCO_3$ (10 mg; 0.12 mmol) in water (1 ml) added and the reaction allowed to proceed for 15 h at 90 °C with vigorous stirring. The reaction was checked by TLC for completion, whence the product was precipitated with addition of water, collected on 42 grade ashless filter paper, and dried in an oven for 1 h at 50 °C.

For the single-spot format, gold-coated glass devices (Section 2.11) were immersed in a solution [5 ml; water, ethanol, DMF, or 70% (v/v) DMF] containing 11-mercapto-1-undecanol (5 m*M*), and allowed to react at room temperature (20 °C) for either 2 or 12 h. The reacted devices were washed

thoroughly and stored in their respective solvent systems at 20 °C. The hydroxylated surfaces were reacted with epichlorohydrin (0.5 *M*) in a sodium hydroxide (0.4 *M*)–diglyme (0.4 *M*) (1:1) mixture for 4 h at 25 °C. After thoroughly washing with water, ethanol, and water again, the surface was immersed in a solution [5 ml; DMF–0.5 *M* NaOH (70:30, v/v)] containing containing amino-ethanethiol-activated ligand (50 μ*M*) and mercaptoethanol (5 m*M*). The devices were allowed to react at 25 °C for 12 h whence they were washed thoroughly in DMF before being stored in ethanol at 20 °C.

For the 10-spot format, the methodology outlined above was followed for making a solution containing the aminoethanethiol-activated ligand (50 μ*M*) and mercaptoethanol (5 m*M*). This solution was then hand spotted, via a P-2 pipette tip, on the gold-coated glass slide in pre-defined linear positions. The solution was allowed to react with the gold surface at 25 °C for 12 h, whence the slide was dipped in DMF (50 ml) to remove unbound ligands. The unreacted epoxide groups were quenched with a solution (5 ml; DMF–0.5 *M* NaOH, 70:30, v/v) containing mercaptoethanol (5 m*M*). The devices were allowed to react at 25 °C for 12 h, whence they were washed thoroughly in DMF before being stored in ethanol at 25 °C.

Gold-coated SPR devices were also incubated in an ethanolic solution (ethanol–water, 20:80, v/v) containing 11-mercapto-1-undecanol (5 m*M*) for 24 h at 25 °C. The hydroxylated surfaces were reacted with epichlorohydrin (0.5 *M*) in a sodium hydroxide (0.4 *M*)–diglyme (0.4 *M*) (1:1, v/v) mixture for 4 h at 25 °C. After thoroughly washing with water, ethanol, and water again, the surface was treated with a basic dextran solution [3.0 g dextran T-500 in 0.1 *M* sodium hydroxide (10 ml)] for 20 h at 25 °C. The resulting chip was rinsed with copious amounts of water, whence the dextran-coated surface was treated with epichlorohydrin (0.5 *M*) in a sodium hydroxide (0.4 *M*)–diglyme (0.4 *M*) (1:1, v/v) mixture for 4 h at 25 °C. After thorough washing with water, ethanol, and water again, the surface was immersed in a solution [5 ml; DMF–0.5 *M* NaOH (70:30, v/v)] containing aminoethanethiol activated ligand (50 μ*M*) and mercaptoethanol (5 m*M*). The devices were allowed to react at 25 °C for 12 h, whence they were washed thoroughly in DMF before being stored in protein binding buffer at 25 °C.

2.13. SPR experiments

All measurements were made using the imaging SPR instrument described in this report. SPR measurements were made by tracking the change in the SPR minima over the time course of the experiment and converting the total minima angle shift to either MI3 or rFVIIa surface loadings expressed in ng/mm^2.

The MI3 protein sample (50–150 μg/ml; 8.4–25.2 μ*M*), in binding buffer (0.1 *M* sodium acetate, pH 4.5), was loaded at 0.25 ml/min for 15–30 min, rinsed with binding buffer for 2 min at 0.25 ml/min, followed by elution with elution buffer (2 *M* acetic acid) at 1 ml/min for 4 min. The chip was rejuvenated with regeneration buffer (30%, v/v, isopropanol–0.2 *M* NaOH) at 1 ml/min for 4 min followed by re-equilibration in binding buffer. This cycle constituted a single run. The concentration of the MI3 protein was increased until saturating conditions were achieved on the SPR device for each ligand within the library and no further signal increase was observed. This concentration was termed the maximum surface coverage concentration. All SPR data are quoted as the mean of triplicate readings unless otherwise stated (mean ± ~ 5%). The SPR device was calibrated for MI3 adsorption/binding using ^{125}I-labelled data and are therefore subject to a further ±5% error margin.

The same general protocol was used for determining the binding and elution profiles for the rFVIIa system except that the binding buffer for this system was 20 m*M* Tris–HCl, 50 m*M* NaCl, 2.5 m*M* calcium chloride, pH 8.0 and the elution buffer was 20 m*M* Tris–HCl, 50 m*M* NaCl, 5 m*M* EDTA, pH 7.5. The rFVIIa protein concentration at which maximum surface coverage was observed was similar for all ligands within the library, 400 μg/ml or 8 μ*M*.

2.14. Determination of K_{AX} for ligands in the single and 10-spot format imaging SPR instrument

The general protocols outlined above were used for determining K_{AX} in the MI3 and rFVIIa systems.

A range of concentrations (four concentrations per ligand; MI3: 5–150 μg/ml; 0.90–25.2 μ*M*; rFVIIa: 10–40 μg/ml; 0.2–0.8 μ*M*) of the protein were tested to establish a relationship between concentration and SPR response (θ_{sp}^{min}). Once these data were gathered, the calculations outlined in [39] were utilised to determine K_{AX}. The concentrations of MI3 and rFVIIa used to determine K_{AX} for each ligand were below the saturating concentration of the SPR device.

2.15. Imaging SPR software platforms and parts

Theoretical modelling of thin films was performed using Thin Film Calc. software (Software Spectra, OR, USA). Beam tracing and lens design was performed using Win Lens software (Spindler and Hoyer, UK). The control of all aspects of the instrument including the National Instruments frame grabber (PCI-IMAQ-1408; Newbury, UK), Pulnix TM-1010 Monochrom CCD camera (Basingstoke, UK), Newport goniometers and motion controller (Newbury, UK), Vector Technologies 635, 670 and 785 nm diode lasers (Arbertillery, UK), and signal analysis/data capture was accomplished using National Instruments LABView software.

The perspex flow cell was designed by Dr. Roger Millington (Cambridge, UK) and engineered by D. Wheatland Engineering (Surrey, UK). The flow cell consisted of a single channel surrounded by a viton O-ring (1.7 cm I.D. and a wall thickness of 1 mm; Nationwide Bearing, UK). A Gilson peristaltic pump (Villiers-Le Bel, France) was used to control the flow-rate throughout the system with PVC tubing (1 mm I.D.) delivering the fluidics. All lenses and prisms were purchased from Spindler and Hoyer.

2.16. Instrumentation

The BioCad 700E Workstation was purchased from Perseptive Biosystems (Boston, MA, USA). The Perkin-Elmer UV–visible lambda 3 spectrophotometer was from Perkin-Elmer Instruments (Buckinghamshire, UK). The ISO-Data 500 multihead γ counter was from I.C.N. Biomedicals (High Wycombe, UK). The pH and conductivity meter, AGB 4000, was purchased from Canterbury Scientific Instruments (Kent, UK). The Edwards Auto306B metal coating system and FTM 7 film thickness monitor were obtained from Bewhay (Hemel Hempsted, UK). The Lucas Dawe ultrasonic bath was from Patterson Scientific (Watford, UK). The rotary evaporator, Buchi RE111, and water bath, Buchi 461, were both purchased from Orme Scientific (Manchester, UK). The freeze drier, Edwards Modulyo, and high vacuum pump, Edwards Pitani 10, were both purchased from Edward High Vacuum (Surrey, UK). The ultracentrifuge, Biofuge Pico, was obtained from Heraeus Instruments (Osterode, Germany). Ultraviolet fluorescence was observed using a Model UVGL-58 light box from UVP (CA, USA).

Molecular modelling, molecular design and all calculations were performed on a Silicon Graphics 4D/35 personal Iris workstation from Silicon Graphics (Reading, UK) loaded with the Quanta97 Software package from Molecular Simulations (San Diego, CA, USA).

2.17. Determination of protein concentration

The protein concentration was routinely measured using the Coomassie dye binding method described by Bradford [40]. The assay was performed according to the manufacturer's protocol and included mixing the on-test protein or standards (100 μl; 0.2–1.4 mg/ml) with 1 ml Coomassie Brilliant Blue G-250 solution (Bio-Rad, CA, USA). After 10 min, the absorbance was measured at 595 nm in a spectrophotometer, and the protein concentration determined by extrapolation from a standard curve created from a range of BSA standards (0.2–1.4 mg/ml).

Protein concentrations were also measured by absorbance at 280 nm. The measured extinction coefficients (1 cm light path) for a 1 mg/ml solution for the relevant proteins were as follows: $A_{280}=1.0$ for MI3 and 1.37 for rFVIIa.

2.18. ^{125}I-Labelling of proteins

MI3 was labelled with ^{125}I according to the iodination method recommended by the reagent supplier. An iodo-bead was washed with 0.1 *M* sodium (2×500 μl) phosphate buffer, pH 6.5, and dried on filter paper. The iodo-bead was added to hot ^{125}I (0.5 mCi, 5 μl) in 0.1 *M* sodium phosphate

buffer (245 μl), pH 6.5 and reacted for 5 min in a lead-wrapped eppendorf vial. An aliquot of MI3 solution (250 μl; 0.40 mg/ml in 0.1 *M* sodium phosphate buffer, pH 6.5) was added to the vial containing the activated ^{125}I and reacted for 8 min at 20 °C. The incorporation of ^{125}I into tyrosine residues of MI3 was stopped by transferring the solution in the reaction vial to a second, lead-wrapped, eppendorf vial to which was added 0.01 *M* sodium iodide (250 μl in 0.1 *M* sodium phosphate buffer, pH 6.5). The iodo-bead in the first vial was washed with 0.1 *M* sodium phosphate buffer, pH 6.5 (250 μl) and the solution combined with the reaction mixture in the second vial. The reaction mixture (1 ml) was then added to the lead-wrapped PD-10 column (equilibrated with 5×5 ml 0.1 *M* sodium acetate buffer, pH 4.5) and 0.1 *M* sodium acetate buffer, pH 4.5 (1.5 ml) was added (total volume 2.5 ml). For each subsequent 0.5 ml of 0.1 *M* sodium acetate buffer, pH 4.5 added, eluted ^{125}I-labelled MI3 fractions were collected (total of 10 fractions) for counting and protein assay.

2.19. Specific activity determination of ^{125}I-labelled protein

The ^{125}I-labelled MI3 protein fractions were counted on a ISO-Data multi-head 500 γ-counter and the five protein containing fractions with the highest number of radioactive counts were pooled, divided into aliquots and frozen for later use. The ^{125}I-labelled MI3 protein concentration was then determined and the specific activity of the ^{125}I-labelled MI3 calculated and expressed in cpm/μg protein.

2.20. Adsorption of ^{125}I-labelled proteins

A perspex immobilisation block, containing glass microscope slide pieces (10 mm×10 mm) coated with a gold layer, was used for all subsequent adsorption experiments. MI3 solutions (100 μl; 1–150 μg/ml in 0.1 *M* sodium acetate, pH 4.5), comprising known amounts of labelled and unlabelled MI3, were added to the reaction chamber with a total adsorption area of 46 mm^2. The adsorption reaction was allowed to proceed for 400 s at 25 °C, whence the gold coated glass pieces were rinsed three times with incubation buffer (100 μl) to remove any loosely bound MI3, removed from the immobilisation block, and counted on a ISO-Data multi-head 500 γ-counter. From this data, the mean surface coverage of MI3 was calculated with respect to the initial concentration added. Preferential adsorption of ^{125}I-labelled MI3 compared to native unmodified MI3 was monitored by adding aliquots (5×100 μl) of MI3 (50–100 μg/ml) containing an increasing amount of ^{125}I-labelled MI3 versus native MI3 (3750, 15 000, 30 000, 60 000, 120 000) to 10 mm×10 mm gold coated glass pieces using the immobilisation protocol described in the previous section.

2.21. Protein adsorption/binding experiments followed by SPR

In order to quantify accurately the amount of protein adsorbed on to a gold coated prism via an SPR measurement, the reflected intensity at a fixed angle or angular shift measurement must be converted to the amount of protein bound (ng/mm^2). This was accomplished by employing the method of [38], where ^{125}I-labelled MI3 adsorption data were combined with reflected intensity or angular shift measurements generated using a similar adsorption protocol.

2.22. Qualitative test for aliphatic amines

The TLC plates were dipped into a solution of ninhydrin (0.2%, w/v) in ethanol and dried with a heat gun until complete development was obtained. The presence of an aliphatic amine was indicated by a brown to purple coloration.

The method for determining free or primary amino groups on beads was developed by Kaiser [41]. A small portion of beads was put in an Eppendorf tube (1.5 ml) and two drops each of the three solutions given below added. The sample is heated to 120 °C in a hot plate for 4–6 min, with a blue colour on the resin indicating the presence of free primary amino groups.

Solution 1: ninhydrin (5 g) in methanol (100 ml).

Solution 2: liquefied phenol (80 g) in ethanol (20 ml).

Solution 3: an aqueous solution (2 ml) of potassium cyanide (0.001 *M*) in pyridine (98 ml).

2.23. Determination of primary amines immobilised on agarose beads using 2,4,6-trinitrobenzenesulfonic acid

The method of Snyder and Sobocinski [42] was used: a small portion (0.50 g moist mass) of the amine-activated gel was washed, its moist mass recorded, and then hydrolysed using HCl (5 *M*; 500 μl) at 50 °C for 10 min. After cooling to 25 °C, the hydrolysed gel slurry was neutralised with NaOH (5 *M*) and the final volume recorded.

TNBS (0.03 *M*; 25 μl) was added to agarose slurry (0.10 g) diluted to 1 ml with sodium tetraborate buffer (0.1 *M*; pH 9.3). The samples were mixed and allowed to stand for 30 min at room temperature prior to measuring the absorbance at 420 nm. The amine content was determined by extrapolation from a standard curve generated using either 6-aminocaproic acid or glycine

2.24. Thin-layer chromatography

Analytical TLC was performed on commercial Macherey–Nagel plates coated with Polygram SIL G/UV$_{254}$ (0.25 mm thick). The sheets were cut to approximate dimensions of 5 cm high×3 cm wide, and samples were spotted 0.5 cm from the base. Migration of samples was allowed to proceed for 4 cm in the appropriate solvent system before being removed from the chamber and allowed to dry. The TLC plate was then examined under an ultraviolet lamp, and the relative position of the spotted samples noted. Further processing of the plate was accomplished by accessing the presence of primary amino groups via exposure to a solution of 0.3% (w/v) ninhydrin in 3 ml acetic acid/100 ml butanol. All sample positions were then converted to R_F values (R_F=position of the sample from baseline/total distance solvent front has moved).

2.25. Mass spectroscopy

Mass spectra were recorded on AEI MS30 or AEI MS50 mass spectrometers [in the fast atom bombardment (FAB) positive mode] at the Chemical Laboratory, Department of Chemistry, University of Cambridge, Cambridge, UK.

3. Results and discussion

3.1. The ligand library

A limited combinatorial library of triazine ligands designed to interact with the two target proteins, MI3 and rFVIIa, was constructed and based on the design principles already enunciated for the target proteins [1,10]. The insulin analogue MI3 contains a hydrophobic dimerisation site composed of several aromatic residues (A:19-Tyr; B:16-Tyr; B:24-Phe; B:25-Phe; B:26-Tyr) which form a broad swathe across the globular protein, with the side chains of residues B:16-Tyr, B:24-Phe and B:25-Phe being particularly exposed to solvent. These residues were selected to create a small combinatorial library of aromatic triazine ligands (Table 1) with characteristics that would allow substantial π–π overlap with the exposed aromatic side chains of B:16-Tyr and B:24-Phe [1]. The ligand library constructed for rFVIIa was based on the 2.0 Å X-ray crystal structure of the tissue factor (TF)–FVIIa complex and identification of putative structures designed to interact with exposed aromatic (4-Phe) and Ca^{2+}-binding γ-carboxyglutamate (Gla) residues (20-Gla) on the prominent Gla-domain of the protein [10]. Key members of the rFVIIa-binding library are represented in the substituents used to construct the combinatorial library on the triazine scaffold (Table 1).

All bis-substituted triazine ligands were synthesised in solution according to the methods described in the Experimental section and characterised by TLC and MS prior to immobilisation on the appropriate solid phase.

3.2. Chromatographic performance of the immobilised ligand library

Fig. 1A shows the screening results for the chromatographic behaviour of MI3 on a 13-member library (Table 1) of immobilised ligands. Analysis of the adsorption and elution characteristics revealed that intentionally designed diversity in the chromato-

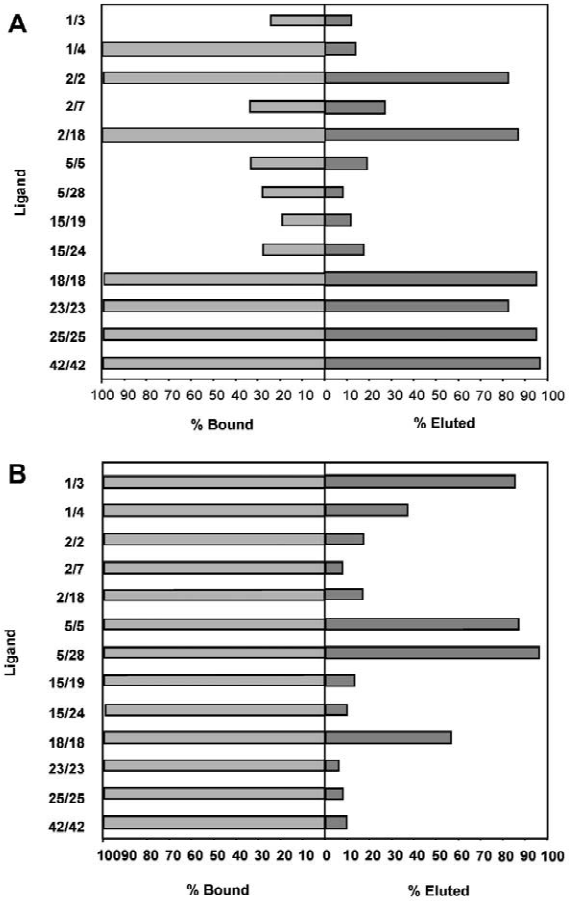

Fig. 1. Initial chromatographic screening of representative examples of the combinatorial library of affinity ligands using (A) MI3 and (B) rFVIIa as the target proteins. The pure protein (1 mg) was loaded onto the immobilised ligand adsorbent (17.5 μmol/g moist mass gel; 1 ml bed volume) equilibrated with 30 column volumes of binding buffer, 0.1 *M* sodium acetate buffer pH 4.5 (MI3) or 20 m*M* Tris, 50 m*M* NaCl, 2.5 m*M* $CaCl_2$, pH 8.0 (rFVIIa). The columns were washed with binding buffer (10 ml) followed by elution with 2 *M* acetic acid (3 ml) (MI3) or 20 m*M* Tris, 50 m*M* NaCl, 5 m*M* EDTA, pH 7.5 (3 ml) (rFVIIa) at 23 °C. The sample, flow through and elution fractions (1 ml) were collected from each column and analysed for the presence of the target protein using the known extinction coefficient. The resulting bound and eluted percentages relate to the total amount of protein loaded on the adsorbent.

graphic behaviour was achieved, despite the apparent similarities in the various ligand structures. The most effective ligands appeared to be symmetrical triazines bis-substituted with amino-naphthols, amino-naphthoic acid and 5-aminoindan, such as 1-amino-5-naphthol (ligand 2/2), 3-amino-2-naphthoic acid (ligand 18/18), 1-amino-7-naphthol (ligand 23/23), 6-amino-1-naphthol (ligand 25/25), and 5-amino-indan (ligand 42/42). Under the conditions selected for the initial screen of the library, typical recoveries of MI3 with these adsorbents were ~60–85%.

Examination of the effect of ligand structure on MI3 binding revealed a high degree of correlation between those ligands comprising 1-amino-naphthalene bearing hydroxylic functions at positions 5, 6 or 7 of the bicyclic nucleus, with recoveries in the range of 60–85%. Conversely, ligands bearing hydroxylic substituents at positions 2 and 4 proved very poor adsorbents, with MI3 recoveries ~10%. The 2-amino-naphthol series displayed a pattern very similar with respect to placement of the hydroxylic substituent. These various ligand isomers were modelled on the graphics workstation which revealed that the bisymmetrical ligands, such as 23/23, displayed more complete π–π overlap with the side chain aromatic rings of residues B:16-Tyr and B:24-Phe than single aromatic ring substituents. However, it is prudent to realise that, not only does the interaction of the protein with the ligand play a crucial role in the binding phenomena, but that the coupling and spacer chemistries, the matrix backbone, and the presentation of the ligand within the dimensionality of the matrix also play vital roles as well. Therefore, the value of computer modelling in visualising the putative interactions between the ligand and the binding interface of MI3, while valuable, should be used solely as a guide and not as a definitive model.

The screening results for the chromatographic recovery of rFVIIa from the library of ligands are shown in Fig. 1B. The most effective ligands were comprised of 3-aminobenzoic acid (5) (Table 1), 1-amino-6-naphthalene sulfonic acid (1), benzylamine (3), 3-amino-2-naphthoic acid (18) and 2-aminobenzimidazole (28). Under the conditions selected for the screen of the library, typical recoveries of rFVIIa with these adsorbents were ~60–95%. Previously published results [10] showed that within this group, the bisymmetric ligand 5/5 and the asymmetric ligand 5/28 showed good binding (over a range of Ca^{2+} concentrations) and recovery (removal of Ca^{2+}) of rFVIIa.

3.3. Determination of the association equilibrium constant (K_{AX})

The equilibrium association constants (K_{AX}) were determined for the library ligands against the target proteins, MI3 and rFVIIa, by the method of Winzor [39]. Examination of Table 2 reveals that despite the similarities in chemical structures of the ligands, there was an almost 1.5-orders of magnitude difference in the association constants between ligand 15/19 ($0.03\pm0.04\cdot10^5$ M^{-1}) and the bis-5-aminoindan ligand 42/42 ($0.50\pm0.64\cdot10^5$ M^{-1}) for the insulin analogue MI3. This performance window, when combined with the data from Fig. 1A, clearly defined the entire range of ligand performance against this protein. Fig. 2A is a compilation of both the elution and association equilibrium constant (K_{AX}) data for this protein. There was a strong indication that those ligands with binding constants $>1.5\cdot10^4$ M^{-1} for MI3 also had recoveries >70% and would be considered for further optimisation [40]. The only exception to this rule appeared to be ligand 1/4, which possessed an equilibrium constant $\sim10^4$ M^{-1}, although a protein recovery of <10%. This result was consistent with the original design strategy which included ligand 1/4 for its inherent high binding capabilities but poor elution properties with respect to MI3. Conversely, those ligands which had binding constants $<10^4$ M^{-1} had generally poor recoveries within the range 5–45%.

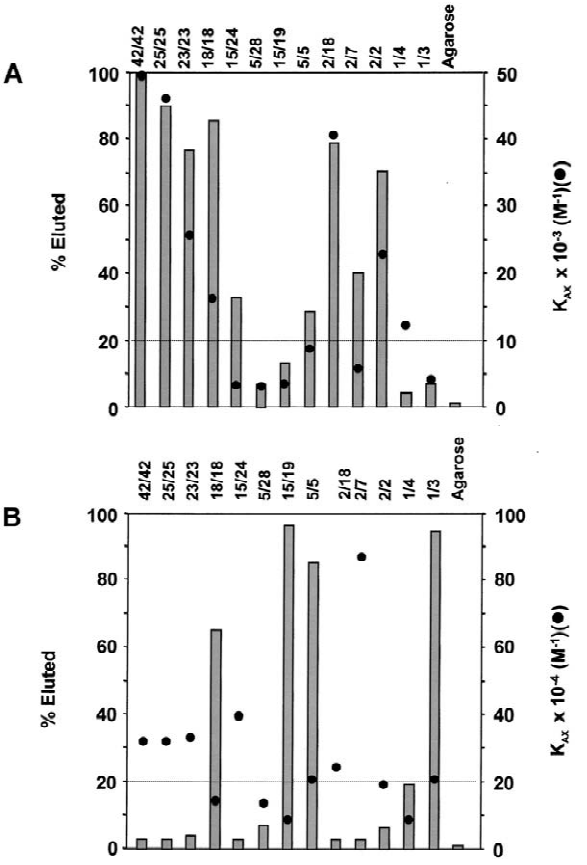

Fig. 2. Compilation showing the elution percentage of (A) MI3 and (B) rFVIIa with the corresponding association equilibrium constant (K_{AX}) for selected members of the combinatorial library.

Table 2
Equilibrium association constants (K_{AX}) (±SD) for the interaction of MI3 and rFVII with immobilised affinity ligands determined chromatographically by the method of Winzor [39]

Ligand	K_{AX} ($\cdot10^{-5}$) (M^{-1})	
	MI3	FVIIa
42/42	0.50±0.64	3.33±0.60
25/25	0.45±0.47	3.24±0.34
2/18	0.41±0.36	2.43±0.23
23/23	0.26±0.23	3.15±0.36
2/2	0.23±0.16	1.90±0.27
18/18	0.16±0.14	1.56±0.15
1/4	0.11±0.12	1.05±0.11
5/5	0.09±0.06	2.01±0.45
2/7	0.06±0.07	8.64±0.58
5/28	0.04±0.05	0.72±0.04
1/3	0.04±0.04	2.20±0.28
15/24	0.04±0.05	3.96±0.48
15/19	0.03±0.04	1.38±0.22

All values represent the mean of triplicate measurements.

The equilibrium association constants (K_{AX}) for the library of immobilised ligands against rFVIIa are also given in Table 2. On cursory examination, this data does not seem nearly as meaningful as the results for MI3. This was in large part because the entire library of ligands were selected for their ability to bind 100% of the target protein (Fig. 1B) with the efficiency of elution becoming the discriminating factor. This apparent tighter binding to the immobilised ligands was reflected in the fact that rFVIIa displayed a substantially higher affinity (K_{AX}) for every member of the library compared to MI3, with relative affinities ranging from 6 to 144-fold. Nevertheless, despite showing equivalent binding charac-

teristics to the adsorbents, analysis of K_{AX} values showed an almost fivefold difference in affinity between rFVIIa and the various members of the library.

The library was designed to display a differential range of binding properties against the two protein systems, MI3 and rFVIIa (Fig. 2A and B). Fig. 2 also shows the elution percentages of the two proteins for all members of the targeted library and shows that there was a spectrum of elution percentages, not only from within each protein system, but between the two target proteins. These data suggest that biomimetic ligand–protein interactions are not simply random hydrophobic or electrostatic events, but display genuine selectivity for the target proteins. This foundation was used as the basis to evaluate the viability of the new SPR screening system and correlation with the chromatographic performance of the same library.

3.4. Instrument design

Fig. 3A shows the SPR instrument with the important design areas highlighted. The imaging system is essentially composed of a metal frame on which two goniometers are mounted around a prism holder. The illumination rail, mounted on the left hand goniometer, contains the illuminating fibre optic (2), polariser, collimating lens, and focusing cylindrical lens. The illuminating fibre optic carries the laser light from the diode lasers (1), located within the temperature-controlled laser housing at the bottom left hand side, through the mode scrambler to the illumination rail. The imaging rail, mounted on the right hand goniometer, contains an additional cylindrical lens (6) and the CCD camera (7). The entire system is controlled through a computer interface (9).

The choice of using diode lasers (1) as the light source was based upon their relatively small size, bright emission, spatially defined beam, specific wavelength, narrow band width and relatively easy coupling into a fibre-optic line. The lasers were housed within a Peltier thermoelectric cooler/heater that precisely controlled the temperature of the diodes. This control was necessary because the angle at which attenuation of light is the greatest (θ_{sp}^{min}) is dependent on wavelength which drifts, with temperature, in laser diodes (typically 0.3 nm/°C). The light was transported from the diode lasers through a lightweight and flexible fibre optic line (2) to the illumination rail. A fibre optic line was chosen for its ability to multiplex different light sources and remove astigmatic properties of diode light to deliver a circularly symmetric beam with a smooth intensity profile. A mode scrambler was used to average the beam paths over the detection time causing the speckle interference pattern created by the coherence property of laser light essentially to blur to a smooth profile (Fig. 3B) (11).

The fibre optic line delivered a bright, coherent, circularly symmetrical beam to the illumination rail that initially polarised the beam to TM for coupling into the surface plasmon mode. From the polariser, the beam entered the collimating achromat lens (3) that collimates the light to deliver a near parallel beam. The focal length and clear aperture of the lens was determined by the distance from the fibre-optic and the diameter of the beam at that distance. The beam then entered the cylindrical lens that focused it in the *x*-axis only through the prism (5) and ultimately on the surface of the gold-coated SPR glass slide. The focal length of the lens was determined by the size of the input beam and the desired range of fan angles (θ). From the cylindrical lens, the beam was launched into the SF2 ($n=1.65$) prism and indexed matched SPR slide to be internally reflected from the gold layer, creating the surface plasmon resonance at the surface of the gold layer. The SF2 prism possessed polished surfaces to allow a 70° internal angle to accommodate all possible θ_{sp} angles within an aqueous environment.

Once the beam was internally reflected from within the prism, it travelled through another cylindrical lens, which focused the collimated beam with respect to the *y*-axis to fit within the boundaries of the CCD detector (7). The camera itself was moved along the imaging rail until the *x*-axis fitted within the detector. The Pulnix TM-1010 Monochrom CCD camera (7) was chosen based on the squareness of the detector geometry, the size of the detector [9.1×9.2 mm; 1008×1008 pixels (800×800 usable)], the ability to control the black/white levels and gain via computer control and the analogue video output, which matched the characteristics of the National Instruments frame grabber.

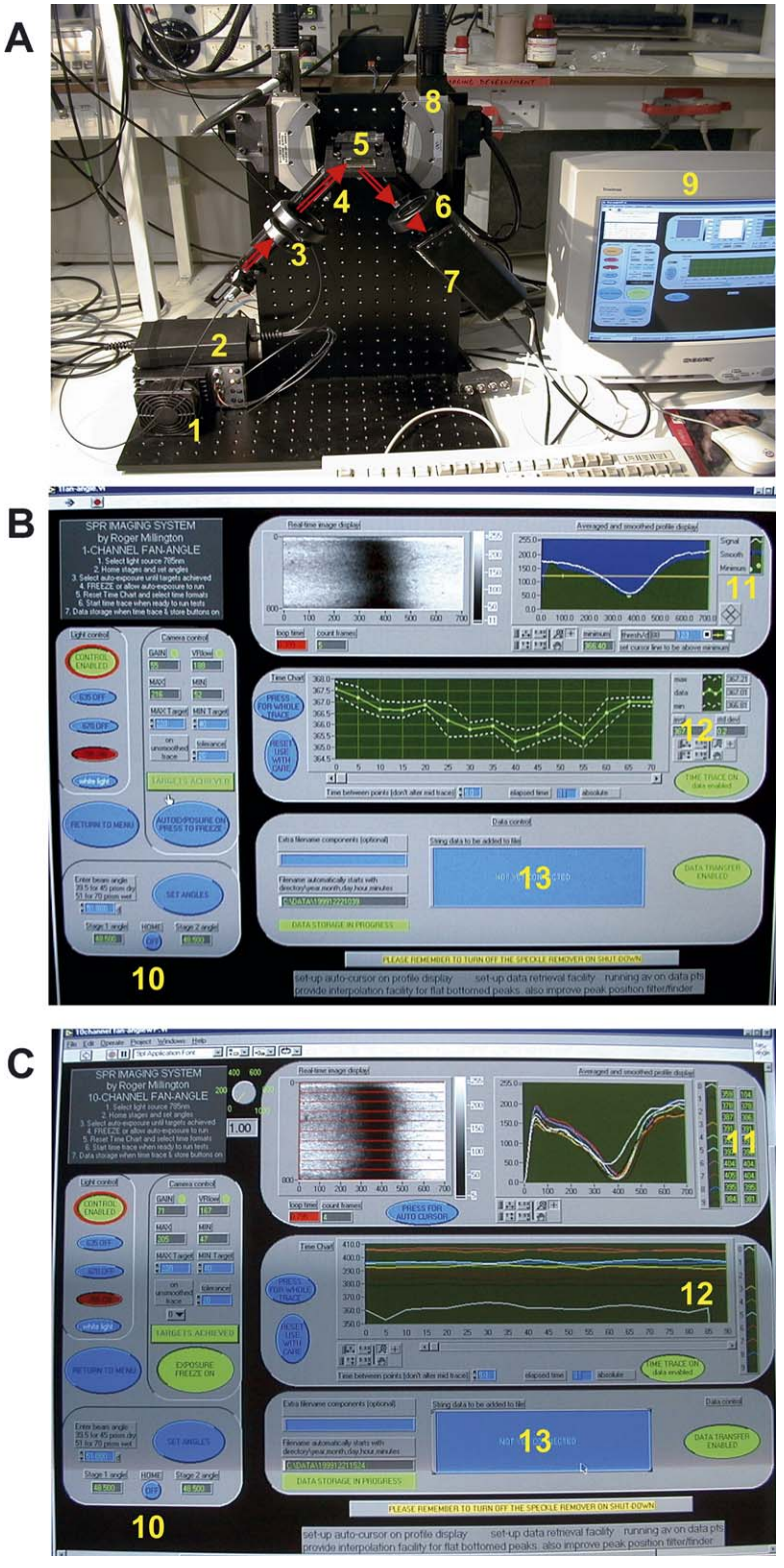
A
1
2
3
4
5
6
7
8
9
B
SPR IMAGING SYSTEM
by Roger Millington
1-CHANNEL FAN-ANGLE
10
11
12
13
C
SPR IMAGING SYSTEM
by Roger Millington
10-CHANNEL FAN-ANGLE
10
11
12
13

The two most important design aspects of the instrument were the refractive index of the prism and the wavelengths of the diode lasers. The interplay between these two parameters essentially determined not only the sensitivity of the instrument, but, ultimately, the spatial resolution of the system. The change of θ_{sp} relative to the change of refractive index ($d\theta_{sp}/dn$) defines the detection sensitivity of the system. The initial choice for the range of wavelengths to use was determined by the correlation between sensitivity and peak definition. As the wavelength of light (λ) gets shorter, the sensitivity increases, but at the expense of the peak width of the SPR minimum (θ_{sp}^{min}) getting broader. This deleteriously affects the peak definition and the ability of the system to locate the precise minimum. Therefore, the choice of the wavelength to use was limited to the red–infrared spectrum (635–785 nm), with a wavelength of 785 nm giving superior peak definition. The amount of sensitivity that is afforded at this wavelength is more than enough for the pg–ng/mm^2 levels of detection that are needed for the protein–biomimetic ligand interaction.

The choice of what refractive index prism to choose was not based solely on sensitivity considerations. For a single beam system in which no spatial recognition over a square area (1 cm×1 cm) is needed, the logical choice would be the BK7 indexed prism (n=1.515). However, theoretical modelling for two-dimensional linear array detection suggested that the prism had to possess the ability, not only to track spatial sites in both a single and multi-beam mode, but also to deliver the best spatially resolved beam of light to the CCD camera.

The interrogation beam is a fan of angles focused to a centre line on the gold-plated SPR device with a width of 1 mm. This beam has the ability to track up to 10 different, linearly arranged sites. The dynamic range of this configuration is not limited by a fixed angle; therefore, θ_{sp}^{min} can be theoretically tracked over any range of angles. However, the optical components were chosen to provide a beam in a fan of angles, which covered a dynamic range encountered within the context of a ligand–protein interaction. For a system in which an entire array of spatially addressable positions needs to be monitored, each linear array of ligands will be provided with a reduced fan of angles or, alternatively, the intensity of the beam at a fixed angle is monitored at each spatial site. In fact, the interrogation beam is collimated and at a fixed angle near θ_{sp}. The intensity change is measured throughout the time course and the dynamic range is determined by how continuous the peak slopes of three different lasers are. The coupling of light into the surface plasmon mode via the Kretschmann configuration, the wavevector equations that describe the incident light and the surface plasmon can be set equal to one another and solved for θ_{sp}:

$$\theta_{sp} = \arcsin\left[\frac{\sqrt{\dfrac{n_m^2 n_s^2}{n_m^2 + n_s^2}}}{n_p}\right]$$

This equation predicts the discrete angle at which surface plasmon coupling will occur based on the refractive index of the sample and system components. The equations that describe wavevector matching include a wavelength dependent term, the dielectric permittivity, ε. Therefore, the dielectric permittivity of the metal, sample and prism will vary with wavelength. This dependence can be exploited when the angle of incidence is fixed and multiple wavelengths of light are sequentially launched into the waveguide/metal film interface. Each wavelength of light has a separate wavevector that describes it and, therefore, the ability to track the ligand–protein interaction through a given range of refractive indices. Numerous groups throughout the last decade [43–45] have studied various facets of

Fig. 3. The CCD-based imaging SPR instrument showing (A) the overall layout of the key components, (B) the graphical interface for the single-spot mode of the instrument, and (C) the graphical interface for the 10-spot mode. The profiles for the resonance peaks were displayed throughout the time course of the experiment, with each time point recorded and displayed as a pixel number. The conversion from pixel to angle was 700 pixels equal to 2.5° angular shift of θ_{sp}^{min} (280 pixels/1° angular shift or 3.5 m°/pixel): (1) diode lasers (635, 670 and 785 nm), (2) fibre optics, (3) lenses, (4) prism, (5) gold SPR device, (6) lens, (7) CCD camera, (8) goniometer, (9) computer control and analysis, (10) diode laser and angle control panel, (11) SPR minimum profile panel, (12) SPR minimum tracking panel, (13) data storage panel.

this method of detection, termed SPR wavelength modulation. Therefore, the choice of prism index is dependent on how smoothly the system can respond to the peak slopes of the three lasers (633, 670 and 785 nm) to yield a continuous dynamic range at a fixed angle. The SF2 ($n=1.65$) indexed prism enables the slope overlay to exist and therefore afford the ability to address potentially 100 sites over a 1 cm$\times$1 cm area. In practice, this particular configuration would monitor the biochemical interaction by relating the change in refractive index by the decrease in intensity (785 nm laser, leading curve). As the refractive index increases, the monitoring is accomplished by the 670 nm laser followed by the 633 nm laser.

The design paradigm for the matching of refractive index and wavelength was shaped by both sensitivity considerations over a broad range of system configurations and dynamic range within a fixed/non-fixed angle environment. To yield the best compromise between all parameters in both configurations, an SF2 indexed prism was chosen, matched to a wavelength range of 635–785 nm. In addition to these properties, the lower angle of incidence (60°) of the SF2 prism, compared with the BK7 prism (70°), reduced the astigmatic properties of the beam rendering better resolution in both spatial axes.

3.5. Calibration of the imaging SPR instrument

In order to quantify accurately the amount of protein adsorbed on to a gold coated prism via the imaging SPR instrument, the reflected intensity at a fixed angle or angular shift measurement must be converted to the amount of protein bound per unit area (ng/mm^2). This was accomplished by using ^{125}I-labelled MI3 adsorption data combined with reflected intensity or angular shift measurements generated using a similar adsorption protocol [38]. Fig. 4 shows the relationship between ^{125}I-labelled MI3 surface loading (ng/mm^2) on a gold-coated glass slide and the corresponding SPR angular shift (θ_{sp}^{min}). Since the imaging SPR instrument was a CCD-based system, the angular change was denoted by a shift in pixels, with a dynamic range of 2.5° or $\sim 2.5 \cdot 10^{-2}$ refractive index units (RIUs), equivalent to 700 pixels. The calibration curve approximates to a surface coverage of 10.10 ± 0.052 ng/mm^2/°.

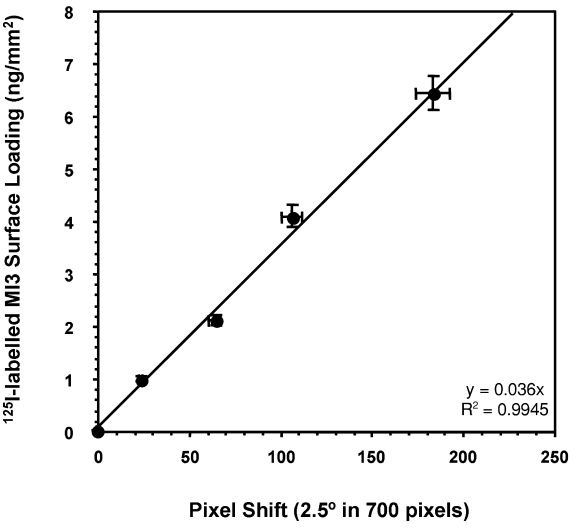

Fig. 4. The relationship between ^{125}I-labelled MI3 surface loading and the corresponding SPR angular shift (θ_{sp}^{min}) on a gold coated glass slide. The relationship approximates a surface coverage of 10.10 ± 0.052 ng/mm^2/° angular shift.

These results agree well with the literature, where the SPR angular shift for a range of proteins approximated to a surface coverage of 10 ng/mm^2/° [46].

Fig. 3B shows the graphical interface that was used to control the key components of the instrument operating with a 785 nm excitation beam, fixed goniometer angle and fan angle measurement for θ_{sp}^{min}.. The attenuated fan angle was displayed as a dark line down the centre of the camera window with an associated pixel number (2.5° maximum measured shift). In this configuration, all 700 usable pixels (CCD), in one axis, were used to average the SPR curve, enabling a smooth, highly resolved, θ_{sp}^{min}. When an interaction occurred, there was a change in the pixel number, resulting in a $\Delta\theta_{sp}^{min}$.

The resolution of SPR-sensing devices has been widely studied by numerous groups [47,48]. For angular based systems, the sensitivity to changes in the refractive index increases with decreasing wavelength [48], whilst for wavelength interrogation and intensity measurements, the sensitivity to changes in refractive index increases with wavelength [47]. In order to ascertain the resolution of the imaging SPR instrument, i.e., the least detectable protein coverage (LDPC), baseline measurements were taken with

both MI3 and rFVIIa binding buffers. The precision of the goniometers (0.001°) did not affect the overall precision for the modes tested because all experiments were performed at a fixed arm angle and the fan of angles were measured (2.5° maximum shift in θ_{sp}^{min}). The mean and standard deviation (in pixels) for the baseline response of a finished SPR device utilising both the MI3 and rFVIIa binding buffers devoid of their respective proteins were determined by measuring θ_{sp}^{min} over a 2 h time course at 3-s intervals for a total of 2400 test points. The resolution, in practice, of the imaging SPR instrument was 0.0022° angular shift in θ_{sp}^{min}, which converted to a protein surface loading of 23 pg/mm^2. This result compares favourably well with the 10–50 pg/mm^2 reported for commercial SPR instruments.

3.6. Screening of the ligand library in single-spot mode

All ligands within the targeted biomimetic library were activated with aminoethanethiol and immobilised on gold-coated glass slides that were indexed matched to the SF2 prism ($n=1.62$). In order to determine both the adsorption and elution percentages for the insulin analogue MI3 to each ligand, the data generated in the chromatographic system (Fig. 1) was used to define the ''high binding'' ligands.

The surface coverage determined by the SPR system for the interaction between ligand 2/2 and MI3 was 1.63 ng/mm^2 (Fig. 5) and very similar to that determined by the single-spot SPR system, 1.45 ng/mm^2. Furthermore, comparison between the SPR and chromatographic systems showed a high degree of correlation between the two data sets. Similar correlations were noted for all other ligands, with three broad ranges of elution percentages being seen (~10, 40–60 and 70–98%). More importantly, the decision as to which ligands to choose for further evaluation proved to be identical for both screening systems. In fact, the correlation of the elution percentages between the chromatographic and SPR systems with respect to the ''high binding'' ligands was remarkably high, with little or no difference being observed. This result was not surprising given that identical linker chemistry was used to attach the ligand to the support in both systems, the supports were both hydrophilic and the design criteria produced biomimetic ligands with a high degree of selectivity and specificity [1]. Therefore, although the chromatographic system presented the ligand immobilised in a three-dimensional agarose bead, and the SPR system rendered the immobilised ligand in a two-dimensional planar configuration, both systems possessed the ability to utilise avidity effects in the binding interaction [49,50].

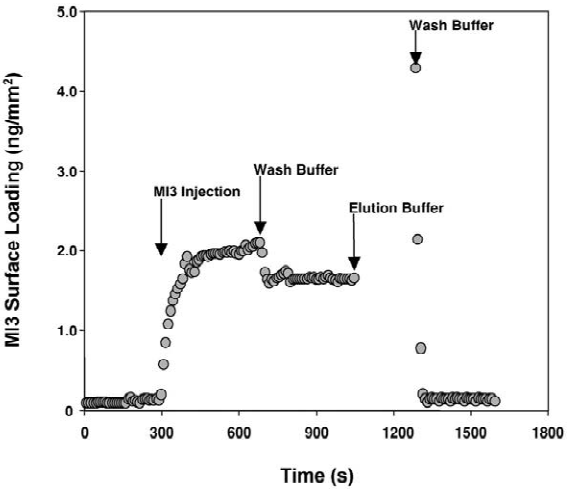

Fig. 5. SPR sensorgram showing the response of a two-dimensional assembly of mercaptoethanol and ligand 2/2. An MI3 surface concentration of 1.63 ng/mm^2 was observed for a 900 s injection of MI3 (50 μg/ml) in 0.1 *M* sodium acetate, pH 4.5. Elution was affected by addition of 2 *M* acetic acid for 240 s, with the response returning to baseline upon addition of binding buffer.

3.7. Determination of K_{AX}

The ability of the imaging SPR system to measure low K_{AX} values ($<1\cdot10^5$ M^{-1}) accurately has been claimed for few commercial instruments, since SPR is much better at measuring high affinity interactions ($>1\cdot10^7$ M^{-1}). As the strength of affinity interactions is reduced, the need for higher concentrations of protein increases, which in turn raises the refractive index of the bulk solution and hence the baseline of the SPR sensorgram for large-molecular-mass proteins. This problem is exacerbated for systems that do not have a large dynamic range for measuring changes in refractive index or where the protein has a high molecular mass.

A range of MI3 concentrations were injected onto

the two-dimensional surfaces with the equilibrium responses measured for the entire library of immobilised ligands. The plateau responses (R_p) were plotted against the plateau responses divided by the concentration of MI3 ($R_p/\overline{C}_A$) with the slope of the resulting Scatchard plot yielding a value for K_{AX} [39]. The Scatchard plot for the interaction between MI3 and ligand 2/2 yields a K_{AX} equal to $7.90\pm0.52\cdot10^4\ M^{-1}$. Whilst this value was 3.5-fold higher than the K_{AX} determined by the column chromatographic format, $2.31\pm0.15\cdot10^4\ M^{-1}$ (Table 2), it was similar to that deduced for the single-spot SPR system, $6.04\pm0.45\cdot10^4\ M^{-1}$. Therefore, three separate analytical systems yielded a similar K_{AX} for the interaction between MI3 and ligand 2/2, thereby allowing the value determined by the SPR system to be used as a good indicator of chromatographic performance.

The K_{AX} values for all of the remaining ligands in the library are listed in Table 3. A plot of K_{AX} values determined by SPR against the equivalent obtained in the column chromatographic format shows a linear relationship between the two systems, with K_{AX} determined in the SPR system being some ~3.0±0.21-fold higher. Comparison of the K_{AX} values and similar data generated for the MI3 chromatographic system suggested that those ligands with binding constants in the range of $>4\cdot10^4\ M^{-1}$ had recoveries >80%. Conversely, those ligands which had binding constants $<4\cdot10^4\ M^{-1}$ had generally poor recoveries within the range from ~5 to 25%.

Table 3
Equilibrium association constants (K_{AX}) (±SD) for the interaction of MI3 and rFVII with immobilised affinity ligands determined by imaging SPR

Ligand	K_{AX} ($\cdot10^{-5}$) (M^{-1})	
	MI3	rFVIIa
42/42	1.293±0.82	6.26±0.23
25/25	1.446±0.74	7.46±0.45
2/18	1.365±0.55	7.42±0.70
23/23	0.600±0.32	7.85±0.62
2/2	0.790±0.29	6.81±0.55
18/18	0.678±0.34	4.37±0.44
1/4	0.496±0.27	6.14±0.24
5/5	0.198±0.21	5.32±0.41
2/7	0.175±0.24	10.3±0.37
5/28	0.105±0.12	2.64±0.15
1/3	<0.100	3.06±0.26
15/24	0.168±0.24	8.28±0.68
15/19	<0.100	5.29±0.38

All values represent the mean of triplicate measurements.

In contrast to the behaviour of MI3, all ligands within the library quantitatively bound rFVIIa. However, the immobilised ligands revealed recovery behaviours with respect to rFVIIa, which fell into the broad ranges of 7–36 and 56–95%. The ligands associated with this latter group were comprised of 3-aminobenzoic acid (5) (Table 1), 1-amino-6-naphthalene sulfonic acid (1), benzylamine (3), 3-amino-2-naphthoic acid (18), and 2-aminobenzimidazole (28). A high degree of correlation was observed between chromatographic and SPR data sets, adding further evidence of the ability of the SPR system to differentiate between the performance of numerous ligands against a particular target protein. Table 3 lists the association equilibrium constants (K_{AX}) for the entire library. As previously observed, this particular set of data does not differentiate between good and poor performing ligands for rFVIIa.

The K_{AX} data generated by SPR correlated with the chromatographic K_{AX} data set rather poorly ($R^2=$ 0.789 rFVIIa versus 0.944 MI3) compared to MI3. However, a clear relationship between the two systems was apparent, with K_{AX} determined in the SPR system being some ~2.5±0.28-fold higher than that determined by chromatography. This result compared favourably with the MI3 system which showed a ~3.0±0.21-fold higher determination for the K_{AX} value.

3.8. The 10-spot mode

Fig. 3C shows the graphical interface that was used to control the key components of the instrument for the 10-spot array. The attenuated fan angles of the ten spatially addressable areas were displayed as a dark line, divided into ten areas, down the centre of the camera window with an associated pixel number for each spot. The 10-spot system had 80 pixels (CCD) devoted to each site for θ_{sp}^{min} smoothing. When an interaction occurred, there was a change in the pixel number for each spatially addressable site, resulting in a $\Delta\theta_{sp}^{min}$.

In order to determine the resolution of the imaging SPR instrument in the 10-spot mode (LDPC),

baseline measurements were taken with the MI3 binding buffer at each of the 10 spatially addressable areas. The resolution of the imaging SPR instrument was found to be 0.0093° angular shift in θ_{sp}^{min}, which converted to a protein surface loading of 97 pg/mm^2. This result showed that there was a ~four-fold decrease in resolution of the instrument in the 10-spot mode compared to the single-spot mode (23 vs. 97 pg/mm^2). This result was not unexpected, since there was a considerable reduction in the number of pixels (80 vs. 800) for smoothing of the θ_{sp}^{min}. Accordingly, the resolution should decrease by approximately the square of 10, the reduction of the pixel count (~3.2). However, this decrease in resolution did not deleteriously effect the results generated with this configuration. The resolution was still well within the necessary sensitivity required for the interactions between the target proteins and biomimetic ligands.

A sub-group of the ligands within the targeted library were chosen to determine the ability of the instrument to generate binding/elution and association equilibrium constant data in the 10-spot mode. Ligands 42/42, 2/18, 1/4, 15/24, and 1/3 were chosen for their differential binding properties against MI3. Each ligand was spotted, in duplicate, in different areas on the linear array to determine not only the reproducibility relative to the single-spot data, but also the reproducibility within the linear array itself. Within the linear array, the reproducibility of the elution percentages was exceptionally good between the five duplicates, with an average mean deviation of $<\pm 2.5\%$. Comparison of the values with the single-spot system showed an average mean deviation of $<\pm 2\%$ for all ligands. Within the linear array, the reproducibility of the K_{AX} values was exceptional between the five duplicates, with the average mean deviation being less than $1 \cdot 10^4\ M^{-1}$. Comparison of the values with the single-spot system generated a near linear correlation, with a small slope bias of 7% for the single-spot system (Fig. 6).

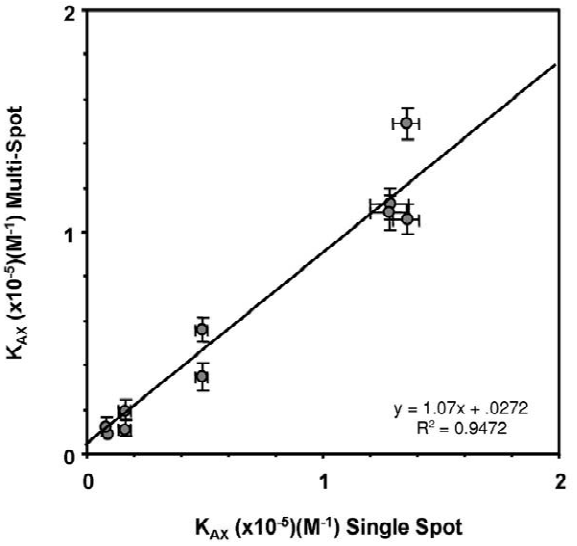

Fig. 6. Comparison of K_{AX} values obtained in both the single-spot mode and the multi-10 spot mode for MI3 binding to selected library members. The relationship was a near linear correlation ($R^2 = 0.9472$; $y = 0.925x$) with a small slope bias of ~7% for the single-spot system (mean±SD).

4. Conclusions

A key objective of this work was to establish a sound foundation on which to build a relational database between the chromatographic behaviour of immobilised ligands and a new imaging SPR screening system. A targeted biomimetic library, comprising 13 ligands from a complete library of ligands [1,10], was synthesised in solution and designed to display a differential range of binding properties against two protein systems, MI3 and rFVIIa. Inspection of Fig. 7 shows that the percentage elution of MI3 and rFVIIa from members of the library determined chromatographically and with the imaging SPR system were broadly comparable for both proteins.

Using ligand 2/2 (Table 1) and MI3 as a model interaction, previously determined in the column chromatographic system [1], two different surfaces were created: first, a two-dimensional surface was fabricated using short and long chain alkyl thiol self-assembled monolayers (SAMs). The functionalised surface generated a maximum coverage of 1.45 ng/mm^2 of bound protein when a 50 μg/ml solution of MI3 was passed over the surface. A second control functionalised surface containing all the components of the first surface except ligand 2/2 gave a response equivalent to a surface coverage of ~0.04 ng/mm^2. This resulted in a signal-to-noise

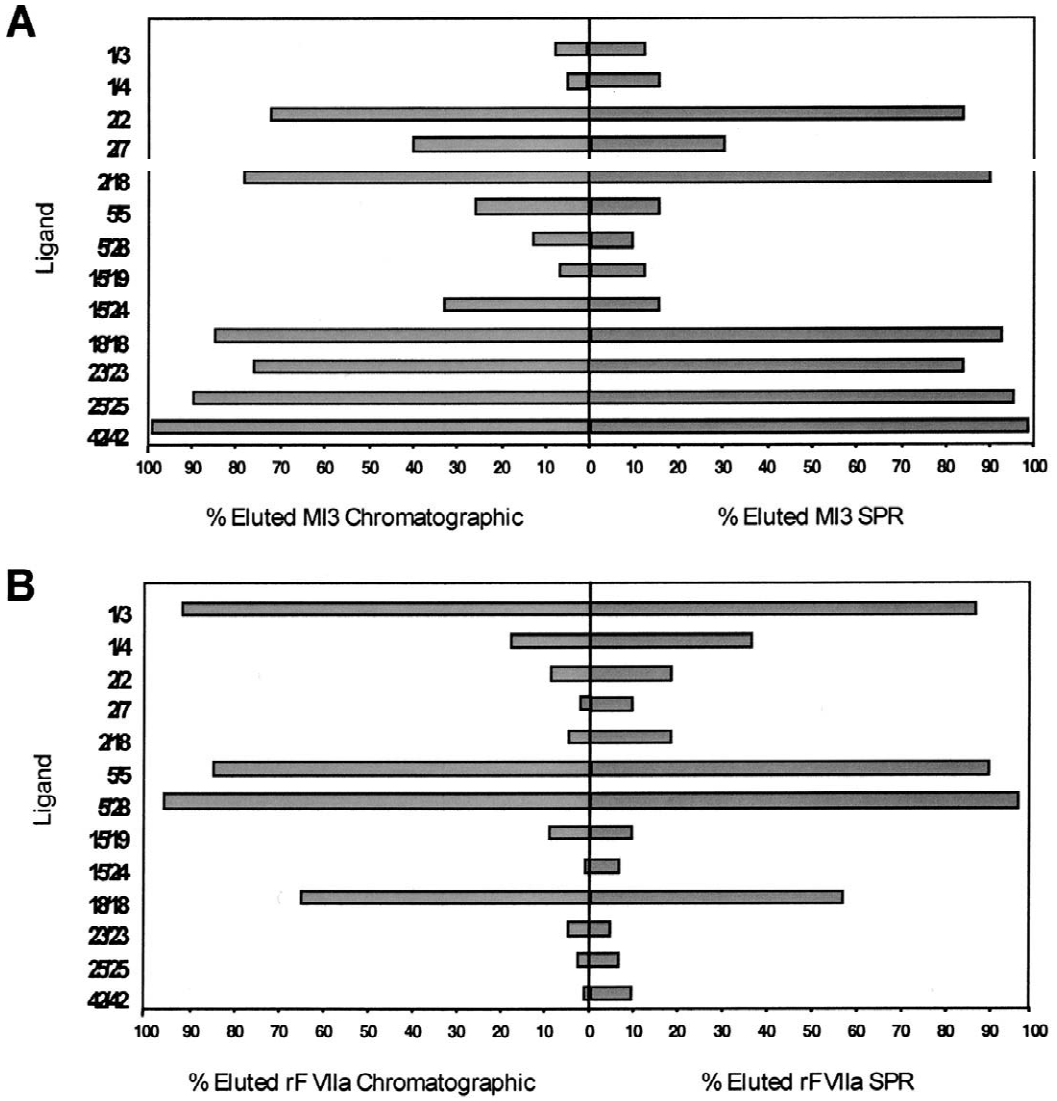

Fig. 7. Comparison of (A) the chromatographic elution percentages for MI3 and rFVIIa with (B) the multi-spot imaging SPR instrument for selected members of the combinatorial affinity library.

ratio of ~35 for the two-dimensional surface. Furthermore, the intrinsic chemical nature of the ligands enables them to be sterilised, depyrogenated, and cleaned-in-place during multiple operational cycles, while retaining their ability to adsorb and elute proteins in quantitative yield [1–11]. The two-dimensional surface was able to withstand the rigours of 100 cycles of treatment with 30% (v/v) isopropanol–0.2 *M* NaOH and autoclaving without any loss of binding capacity. The association equilibrium constant (K_{AX}) measured for a two-dimensional immobilised ligand 2/2 surface interacting with MI3 yielded a value of $6.04 \pm 0.45 \cdot 10^4\ M^{-1}$, closely matching the $2.31 \cdot 10^4\ M^{-1}$ value generated for this interacting pair in the column chromatographic format.

Secondly, a three-dimensional deposition of immobilised ligand was accomplished by employing an

extended polymer matrix comprising a dextran hydrogel [20,21]. In addition to its minimal non-specific protein adsorption, dextran offered increased signal-to-noise ratios compared to the two-dimensional surfaces [38,41] and the ability of the matrix to present the ligand in a geometry more closely resembling the column chromatographic format. A three-dimensional surface composed of a dextran hydrogel and ligand 2/2 generated a maximum coverage of 2.30 ng/mm^2 of bound protein when a 50 μg/ml solution of MI3 was passed over the surface. A control functionalised surface containing all the components of the first surface except ligand 2/2 [38] generated a surface coverage of ~0.02 ng/mm^2. This resulted in a signal-to-noise ratio of ~114, a ~3.3× increase over the two-dimensional chip. However, while the three-dimensional dextran/ligand 2/2 surface did offer an increased signal response over the two-dimensional surface, it suffered from poor durability and was unable to withstand either the rigorous cleaning or the sterilisation procedures [38]. The K_{AX} measured for the three-dimensional immobilised ligand 2/2 surface interacting with MI3 was $4.72 \pm 0.24 \cdot 10^4\ M^{-1}$; this value agreed well with the value generated for this system in the column chromatographic format. Therefore, based upon the overall performance of the two surfaces, the two-dimensional assembly was chosen as the format to evaluate the performance of the remaining ligands in the targeted biomimetic library by the imaging SPR screening system, since the synthesis was more facile and the surface more robust.

The SPR data generated for the MI3 association equilibrium K_{AX} values were comparable to the values obtained in the chromatographic system. These data were plotted against one another and generated a nearly linear relationship ($R^2 = 0.944$) with a slope bias of ~3.0±0.21-fold higher for the SPR system. In contrast to MI3, rFVIIa did not generate as good a regression value ($R^2 = 0.789$ [rFVIIa]; $R^2 = 0.944$ [MI3]). However, a linear relationship between the two systems was apparent, with K_{AX} values determined in the SPR system being ~2.5±0.28-fold higher. Furthermore, when the rFVIIa data was combined with the MI3 data to generate the final relational correlation for K_{AX} values, between the chromatographic and SPR imaging systems, a nearly linear relationship ($R^2 = 0.875$) with a slope bias of ~2.5±0.25-fold higher for the SPR system was generated (Fig. 8). A potential explanation for the slope bias between the two systems concerns the partition coefficient between the protein solute and the ligands immobilised on the agarose beads in the chromatographic system and the potential for significant avidity between the proteins and ligands immobilised to two- and three-dimensional matrices. The equations that were used to determine K_{AX} for this system did not take into account these parameters, resulting in equilibrium constant values that could possibly be underestimated [39]. The K_{AX} value generated in the SPR system would be less likely to be influenced by these factors since it was a two-dimensional rather than a three-dimensional surface. This contention is strengthened by the fact that the K_{AX} value generated for the three-dimensional ligand 2/2-dextran layer ($4.72 \pm 0.24 \cdot 10^4\ M^{-1}$) in the SPR system was somewhat closer to the chromatographic value ($2.31 \cdot 10^4\ M^{-1}$) for this interacting pair than the two-dimensional ($6.04 \pm 0.45 \cdot 10^4\ M^{-1}$) SPR system. However, an alternative explanation is that since the evanescent

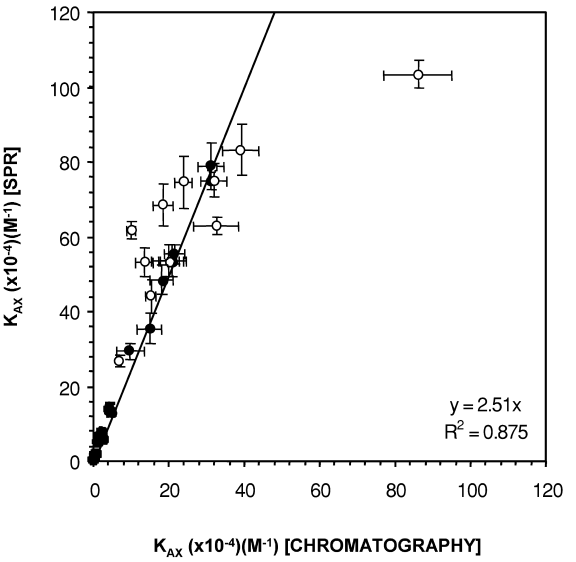

Fig. 8. K_{AX} correlation between the chromatographic and imaging SPR systems for both protein targets, MI3 (●) and rFVIIa (○). The relationship was approximately linear ($R^2 = 0.875$) with the SPR values ~2.5-fold higher ($y = 2.51x$). All points represent the mean of triplicate measurements (mean±SD).

wave of the SPR device decays exponentially into the liquid medium and thus interrogates only the environment immediately adjacent to the optical surface, adsorbed protein molecules proximal to a two-dimensional surface will be more readily ''seen'',and thus appear to have an apparently higher affinity, than those bound to the distal regions of a three-dimensional dextran layer.

Finally, the putative 10-spot mode was evaluated for a linear array of 10 spatially addressable sites. These sites contained five different ligands, in duplicate, within the targeted library, which were evaluated for binding/elution and K_{AX} values. The 10-spot mode displayed almost identical performance to the single-spot mode using both criteria. Moreover, the correlation of the K_{AX} values generated a near linear relationship ($R^2 = 0.947$) with a small slope bias of 7% for the 10-spot mode.

Few groups have demonstrated a true multi-channel SPR system capable of monitoring numerous sites both simultaneously and independently. Commercial instruments with four and eight channels, respectively, based on detection with a photodiode array to interpolate the change in reflected intensity, have the ability to read each channel simultaneously, resolve surface coverages of 10 pg/mm^2 and measure K_{AX} values in the range of 10^4 to 10^9 M^{-1}, have been introduced. Two prototype instruments, based on a true CCD-based SPR imaging system, have been revealed in the literature to have the ability to spatially address nine [51] and 16 spots [52] simultaneously, although the data, in both instances, is superficial, and shows only that both systems can qualitatively measure the binding of a protein to a functionalised surface.

In summary, the SPR imaging system reported here displayed near equivalent performance to a conventional chromatographic system. The ligands within the targeted biomimetic library chosen for further evaluation were identical in both systems. The amount of protein and time that was needed to complete a typical screen of a biomimetic ligand in the SPR system was approximately 0.50 mg and 1 h compared to almost 65 mg and 5 h for the chromatographic system. This 130-fold reduction in the amount of protein consumption coupled with the fivefold reduction in the amount of time necessary to screen a ligand, suggests that the imaging SPR system may become the screening methodology of choice for biomimetic ligands. Furthermore, these reductions in time and target protein consumption were enhanced in the 10-spot mode, where the evaluation of five duplicate ligands essentially took the same time as a single ligand in the single-spot mode.

Although the present imaging SPR system has only been tested in the 10-channel mode, this instrument does possesses the potential for addressing up to thousands of sites simultaneously. The area that can be comfortably imaged (~1 cm^2) coupled with the minimum area needed to image one site (100 μm^2) [52], indicates the potential for spatially addressable sites that could be available for biomimetic ligand screening. In principle, these areas could be functionalised with ligands utilising ink jet technology [53], which would allow for precise and reproducible positioning of the functionalising chemistry. This SPR imaging system would be a significant leap forward, over current prism-coupled systems, for direct, optical-based, high throughput monitoring.

Acknowledgements

The authors would like to thank J. Christiensen, I. Mollerup, H. Valore and K.R. Hejnæs of Novo Nordisk A/S for being a delight to work with and for financial support.

References

[1] K. Sproule, P. Morrill, J.C. Pearson, S.J. Burton, K.R. Hejnæs, H. Valore, C.R. Lowe, J. Chromatogr. B 740 (2000) 17.
[2] C.R. Lowe, A.R. Lowe, G. Gupta, J. Biochem. Biophys. Methods 49 (2001) 561.
[3] R.-X. Li, V. Dowd, D.J. Stewart, S.J. Burton, C.R. Lowe, Nat. Biotechnol. 16 (1998) 190.
[4] S.F. Teng, K. Sproule, A. Hussain, C.R. Lowe, J. Mol. Recognit. 12 (1998) 67.
[5] U.D. Palanisamy, A. Hussain, S. Iqbal, K. Sproule, C.R. Lowe, J. Mol. Recognit. 12 (1998) 57.
[6] U.D. Palanisamy, D.J. Winzor, C.R. Lowe, J. Chromatogr. B 746 (2000) 265.
[7] S.F. Teng, K. Sproule, A. Hussain, C.R. Lowe, J. Chromatogr. B 740 (2000) 1.

[8] H. Filippusson, L.S. Erlendsson, C.R. Lowe, J. Mol. Recognit. 13 (2000) 370.
[9] N.P. Burton, C.R. Lowe, J. Mol. Recognit. 6 (1993) 31.
[10] P.R. Morrill, G. Gupta, K. Sproule, D. Winzor, J. Cristensen, I. Mollerup, C.R. Lowe, J. Chromatogr. B 774 (2002) 1.
[11] C.R. Lowe, Curr. Opin. Chem. Biol. 3 (2001) 248.
[12] M. Divers, J. Biomol. Screening 4 (1999) 177.
[13] R.M. Eglen, J. Biomol. Screening 4 (1999) 179.
[14] S. Fox, S. Farr-Jones, M.A. Yund, J. Biomol. Screening 4 (1999) 183.
[15] C.R. Lowe, D.C. Cullen, E. Gizeli, N.J. Goddard, L.D. Gray-Stephens, P. Maynard, B.F.Y. Yon Hin, Clin. Biochem. Rev. 13 (1992) 22.
[16] C.R. Lowe, Curr. Opin. Chem. Biol. 3 (1999) 106.
[17] B. Liedberg, C. Nylander, I. Lundström, Sens. Actuators 4 (1983) 299.
[18] M.T. Flanagan, R.H. Pantell, Electron. Lett. 20 (1984) 968.
[19] D.C. Cullen, R.G.W. Brown, C.R. Lowe, Biosensors 3 (1987/1988) 211.
[20] U. Jonsson, L. Fagerstam, B. Ivarsson, B. Johnsson, R. Karlsson, K. Lundh, S. Lofas, B. Persson, H. Roos, I. Ronnberg, S. Sjölander, E. Stenberg, R. Stahlberg, C. Urbaniczky, H. Ostlin, M. Malmqvist, Biotechniques 11 (1991) 620.
[21] B. Johnsson, S. Lofas, G. Lindquist, Anal. Biochem. 198 (1991) 268.
[22] B. Liedberg, C. Nylander, I. Lundström, Biosens. Bioelectron. 10 (1995) R1.
[23] D. Neri, S. Montigiani, P.M. Kirkman, Tends Biotechnol. 14 (1996) 465.
[24] G.W. Oddie, L.C. Gruen, G.A. Odgers, L.G. King, A.A. Kortt, Anal. Biochem. 244 (1997) 301.
[25] T. Turbadar, Proc. Lond. Phys. Soc. 73 (1958) 40.
[26] A. Otto, Physics 216 (1968) 398.
[27] E. Kretschmann, H. Raether, Z. Naturforsch. 23 (1968) 2135.
[28] S.R. Karlsen, K.S. Johnston, R.C. Jorgenson, S.S. Lee, Sens. Actuators B 25 (1995) 747.
[29] L.G. Fagerstam, A. Frostellkarlsson, R. Karlsson, B. Persson, I. Ronneberg, J. Chromatogr. 597 (1992) 397.
[30] R. Karlsson, A. Michaelsson, L. Mattsson, J. Immunol. Methods 145 (1991) 229.
[31] K. Matsubara, S. Kawata, S. Minami, Appl. Optics 27 (1988) 1160.
[32] A.H. Severs, R.B.M. Schasfoort, M.H.L. Salden, Biosens. Bioelectron. 8 (1994) 185.
[33] C. Jung, S. Lee, K. Kuhn, Appl. Optics 34 (1995) 946.
[34] H.E. Debruijn, R.P.H. Kooyman, J. Greve, Appl. Optics 32 (1993) 2426.
[35] H. Morgan, D.M. Taylor, Appl. Phys. Lett. 64 (1994) 1330.
[36] M.N. Zervas, I. P Giles, Electron. Lett. 25 (1989) 321.
[37] H.E. Debruijn, B.S.F. Altenburg, R.P.H. Kooyman, J. Greve, Optics Commun. 82 (1991) 425.
[38] D.M. Disley, P.R. Morrill, K. Sproule, C.R. Lowe, Biosens. Bioelectron. 14 (1999) 481.
[39] D.J. Winzor, J. Chromatogr. A 803 (1998) 291.
[40] M. Bradford, Anal. Biochem. 72 (1976) 248.
[41] E. Kaiser, Anal. Biochem. 34 (1970) 595.
[42] S.L. Snyder, P.Z. Sobocinski, Anal. Biochem. 64 (1975) 284.
[43] A. Hanning, J. Roeraade, J.J. Delrow, R.C. Jorgenson, Sens. Actuators B 54 (1999) 24.
[44] K.S. Johnston, K.S. Karlsen, C.C. Jung, S.S. Lee, Mater. Chem. Phys. 42 (1995) 242.
[45] R.C. Jorgensen, S.S. Lee, Sens. Actuators A 43 (1994) 44.
[46] E. Stenberg, B. Persson, H. Roos, C. Urbaniczky, J. Colloid Interf. Sci. 143 (1991) 513.
[47] J. Homola, Sens. Actuators B 41 (1997) 207.
[48] J. Homola, I. Koudela, S.S. Lee, Sens. Actuators B 54 (1999) 16.
[49] E.M. Gordon, R.W. Barrett, W.J. Dower, S.P.A. Fodor, M.A. Gallop, J. Med. Chem. 37 (1994) 1385.
[50] J.D. Andrade, V. Hladky, Adv. Polym. Sci. 79 (1986) 1.
[51] J.M. Brockman, A.G. Frutos, R.M. Corn, J. Am. Chem. Soc. 121 (1999) 8044.
[52] C.E.H. Berger, T.A.M. Beumer, R.P.H. Kooyman, J. Greve, Anal. Chem. 70 (1998) 703.
[53] J. Kimura, Y. Kawana, T. Kuriyama, Biosensors 4 (1989) 41.